Article:
Bai, L, Guo, J, Lin, G et al. (2015) Steady-state modeling and analysis of a loop heat pipe under gravity-assisted operation. APPLIED THERMAL ENGINEERING, 83. pp. 88-97. ISSN: 1359-4311

https://doi.org/10.1016/j.applthermaleng.2015.03.014

Steady-state modeling of a loop heat pipe in gravity-assisted operation

Lizhan Bai[1,*], Jinghui Guo[1], Guiping Lin[1], Jiang He[2], Dongsheng Wen[3]

1 Laboratory of Fundamental Science on Ergonomics and Environmental Control, School of Aeronautic Science and Engineering, Beihang University, Beijing 100191, PR China

2 Beijing Key Laboratory of Space Thermal Control Technology, Beijing Institute of Spacecraft System Engineering, Beijing 100094, PR China

3 School of Chemical and Process Engineering, University of Leeds, Leeds, LS2 9JT, UK

Abstract: In this paper, a steady-state mathematical model of a loop heat pipe (LHP) in gravity-assisted operation has been established based on two driving modes: gravity driven mode and capillarity-gravity co-driven mode. The modeling results show good agreement with experimental data, and the operating characteristics of the LHP under gravity-assisted attitude has been theoretically investigated. When the heat load applied to the evaporator is smaller than the transition heat load, the LHP is operating in the gravity driven mode, the working fluid in the vapor line is in the two-phase state due to the existence of additional liquid mass flow, and the operating temperature is obviously lower than that under horizontal or adverse elevation attitudes caused by reduced heat leak from the evaporator to the compensation chamber and enhanced cooling of the return liquid to the compensation chamber. In addition, the effect of positive elevation on the steady-state operating temperature and thermal conductance of the LHP is analyzed. This study contributes to the comprehensive understanding of the operating principle and characteristics and can guide the design of LHPs in terrestrial surroundings.

Keywords: loop heat pipe; mathematical model; driving mode; operating characteristics; experiment

* Corresponding author. Tel.: +86 10 8233 8600; Fax: +86 10 8233 8600
E-mail address: bailizhan@buaa.edu.cn (L. Bai).

1. INTRODUCTION

Loop heat pipes (LHPs) are effective and efficient two-phase heat transfer devices that utilize the evaporation and condensation of a working fluid to transfer heat, and the capillary forces developed in fine porous wicks to circulate the working fluid[1, 2]. Their high pumping capability and superior heat transport performance have been traditionally utilized to address the thermal-management problems of spacecraft, and were successfully applied in many space tasks[3-7]. More recently, its application has been extended to terrestrial surroundings such as in electronics cooling[8-10] and thermal-management systems for aircraft and submarines[11-14]. Their long distance heat transport capability and flexibility in design could offer many advantages compared with traditional heat pipes and other heat transfer devices.

So far, quite a few studies on the mathematical modeling of LHPs have been conducted, which revealed some working principles and operating characteristics of LHPs[15-22], as briefly reviewed below . Ref.[15] established a 1-D steady-state mathematical model of a LHP, which could reflect the variable conductance characteristics of the LHP, but the oversimplification in calculating the radial conductance of the wick and two-phase pressure drop in the condenser brought large difference between the modeling and experimental results. Improved treatment on the two-phase pressure drop in the condenser was conducted in Ref.[16], where five different two-phase pressure drop correlations were assessed and better predictions were achieved. The modeling of the radial conductance of the evaporator wick was improved in Ref.[17] by solving a radial 1-D energy equation, in which the effect of the fluid convection was considered. Ref.[18] developed a comprehensive steady-state model, and showed good predictions when the evaporator was horizontal with or higher than the condenser, but large deviation from the experimental results was observed at the gravity-assisted mode . Further improvement of was attempted in Ref.[19] where the

liquid/vapor interface in the condenser and the void fraction in the compensation chamber (CC) were considered . Ref.[20] developed a steady-state mathematical model of a LHP by considering the evaporator wick as either single-layer or two-layer composite structures, and the condenser having the annular flow pattern. The effects of surface tension of liquid and the interaction between the liquid and vapor phases in the condenser, including both frictional and momentum-transfer shear stresses, were considered. The model revealed the observed conductance reduction when LHPs operate under the constant conductance mode, which cannot be predicted by traditional models. Ref.[21] conducted a numerical analysis based on a 2-dimensional dynamic mesh model to include the influence of non-uniform heat load on the performance of a flat-plate evaporator inside a LHP. The variations of evaporation heat transfer coefficient, outflow working fluid temperature, vapor and liquid interface position, and surface temperature at different heat loads were analyzed. In Ref.[22], a mathematical model of the startup process of a LHP was established based on the node network method, and a parametric analysis including the effects of startup heat load, thermal capacity of the evaporator and compensation chamber, heat sink temperature and ambient temperature on the startup characteristics of the LHP were conducted.

To the best of our knowledge, the mathematical models presented above are only applicable to the situation when the evaporator is horizontal with or higher than the condenser of the LHP. However, when the LHP is operating under the gravity-assisted attitude, i.e. the condenser is located higher than the evaporator, large deviations are expected. . Experimentally, Ref.[23] showed that the operating temperature exhibited distinctive features when the LHP was operating under the gravity-assisted attitude. A gravity-assisted operating theory was proposed, which categorized the steady state operation into capillary-controlled and gravity-controlled modes, to better explain the results. However theoretical investigation of the LHP operation under gravity-assisted mode is still lacking . With the rapid development

of LHPs for terrestrial applications, it is of high interest to establish accurate mathematical models for gravity-assisted LHPs and to better understand their operating principle and characteristics, and guide the engineering design, which forms the objective of this study.

2. MATHEMATICAL MODELING

2.1 Two driving modes

When the LHP is operating under horizontal or adverse elevation attitudes, the capillary force generated by the evaporator wick is the driving source for the circulation of the working fluid in the loop. However, when the LHP is operating under the gravity-assisted attitude, the situation becomes much different and very complicated. As reviewed above, two driving modes could be observed under gravity-assisted mode[23, 24]: gravity-driven mode and capillarity-gravity co-driven mode, depending on the applied heat load. At a low heat load, LHP tends to operate in the gravity-driven mode where the gravity is the dominant driving source for the circulation of the working fluid. Under such a condition, the working fluid in the vapor line is in the two-phase state due to the existence of additional liquid mass flow, and no clear liquid/vapor interface exists at the outer surface of the evaporator wick, as shown in Fig.1(a). At a high heat load, , LHP operates in the capillarity-gravity co-driven mode, where the capillary force and gravity are both driving sources for the circulation of the working fluid The working fluid in the vapor line is pure vapor, and there is a clear liquid/vapor interface at the outer surface of the evaporator wick, as shown in Fig.1(b).

2.2 Determination of the transition heat load

To realize the steady-state modeling of a LHP in gravity-assisted operation, the first and most important step is to determine the transition heat load (Q_{tr}), i.e, the heat load that responsible for the transition from the gravity mode to

capillarity-gravity model. At the transition heat load, the working fluid in the vapor line is pure vapor, and the gravitational pressure head generated in the liquid line just satisfies the requirement to drive the circulation of the working fluid along the loop, so the pressure balance equation can be expressed as:

$$\int_{ll} \rho_l \, g \, dH = \Delta P_{vg} + \Delta P_{vl} + \Delta P_c + \Delta P_{ll} + \Delta P_{wi} \quad (1)$$

Because the gravitational pressure head in the liquid line and the frictional pressure drop in each component of the LHP are both strong functions of the operating temperature, the steady-state operating temperature is initially unknown. It is impossible to directly calculate the transition heat load based on equation (1), and the transition heat load and the steady-state operating temperature should be obtained simultaneously, as schematically shown in Fig.2, and briefly introduced below.

1) Calculation of the heat transfer and pressure drop in each component of the LHP, which is the same as that in our previous mathematical model [20], and is not repeated here.

2) In the solution process, a relatively large heat load as the transition heat load is firstly specified,. In general, the specified relatively large heat load can be simply determined based on that the gravitational pressure head in the liquid line where the liquid is at the lowest temperature i.e. the heat sink temperature is equal to the frictional pressure drop in the vapor line where the vapor is at the possible highest saturation temperature.

3) By decreasing the transition heat load gradually and calculating the temperature distribution along the loop, the total pressure drop along the loop will be just balanced by the gravitational pressure head generated in the liquid line. Under this condition, the actual transition heat load and the steady-state operating temperature can be obtained simultaneously.

2.3 Gravity driven mode

When the heat load applied to the evaporator is smaller than the transition heat load, LHP operates in the gravity-driven mode. The gravitational pressure difference between the liquid line and vapor line is the driving source for the circulation of the working fluid along the loop, so the pressure balance equation can be expressed as:

$$\int_{ll} \rho_l \, g \, dH - \int_{vl} \bar{\rho} \, g \, dH = \Delta P_{vg} + \Delta P_{vl} + \Delta P_c + \Delta P_{ll} + \Delta P_{wi} \tag{2}$$

where

$$\bar{\rho} = \rho_v \alpha + \rho_l (1 - \alpha) \tag{3}$$

$$\alpha = \frac{x \rho_l}{x \rho_l + (1 - x) \rho_v S} \tag{4}$$

Generally, the vapor mass flowrate in the vapor line in the gravity driven mode is relatively small, and the flow pattern in the vapor line is mainly bubbly or slug flow. For simplification purpose, homogeneous flow model is adopted here, and the slip ratio (S) can be set as 1.0 accordingly. By substituting equation (4) into equation (3), the average density of the working fluid in the vapor line can be expressed as:

$$\bar{\rho} = \frac{\rho_l \rho_v}{x \rho_l + (1 - x) \rho_v} \tag{5}$$

In the gravity driven mode, as the working fluid in the vapor line is in the two-phase state, the actual mass flowrate of the system at the inlet of the vapor line becomes:

$$\dot{m} = \dot{m}_v + \dot{m}_l \tag{6}$$

Based on the energy conservation, the vapor mass flowrate at the inlet of the vapor line can be expressed as:

$$\dot{m}_v = \frac{Q_{ap} - Q_{hl} - Q_{hw}}{\lambda} \tag{7}$$

Because the pressure drop in each component is directly related to the mass flowrate, the liquid mass flowrate at the inlet of the vapor line naturally adjusts itself to match the pressure balance as shown in equation (2) under a steady-state condition.

Because the working fluid in the vapor line is in the two-phase state, the heat transfer between the working fluid in the vapor line and the ambient is in the form of latent heat, and the energy equation of the vapor line can be expressed as follows by neglecting the small thermal conduction through the pipe wall:

$$-\dot{m}\frac{dh}{dL} = \left(G / L\right)_{vl-a}\left(T - T_a\right) \tag{8}$$

As the enthalpy value depends on the selection of the initial state at which the enthalpy is zero, the enthalpy of the saturated liquid with respect to the local pressure is set zero here, and the enthalpy value of the working fluid at different states then can be expressed as:

$$h = \begin{cases} \lambda + C_{pv}(T - T_{sat}) & (T > T_{sat}) \quad \text{superheated vapor} \\ \lambda x & \left(T = T_{sat}\right) \quad \text{two-phase state} \\ C_{pl}(T - T_{sat}) & (T < T_{sat}) \quad \text{subcooled liquid} \end{cases} \tag{9}$$

Accordingly, the temperature and vapor quality at different states can be calculated as:

$$T = \begin{cases} (h - \lambda) / C_{pv} + T_{sat} & \text{superheated vapor} \\ T_{sat} & \text{two-phase state} \\ h / C_{pl} + T_{sat} & \text{subcooled liquid} \end{cases} \tag{10}$$

$$x = \begin{cases} 1 & \text{superheated vapor} \\ h / \lambda & \text{two-phase state} \\ 0 & \text{subcooled liquid} \end{cases} \tag{11}$$

For the two-phase flow, the pressure drop in the vapor line consists of three components: frictional, acceleratory and gravitational pressure drop. Based on the homogeneous flow assumption , the pressure drop in the vapor line can be expressed as:

$$-\left(\frac{dP}{dL}\right)_{vl} = -\left(\frac{dP_f}{dL}\right)_{vl} - \left(\frac{dP_a}{dL}\right)_{vl} - \left(\frac{dP_g}{dL}\right)_{vl} = \frac{P}{A}\tau + \left(\frac{\dot{m}}{A}\right)^2 \frac{d\overline{v}}{dL} + \overline{\rho} g \sin\theta \tag{12}$$

where

$$\tau = f \frac{1}{2\overline{\rho}}\left(\frac{\dot{m}}{A}\right)^2 \tag{13}$$

To realize the smooth transition of the frictional factor from laminar to turbulent flow, the frictional factor is

calculated as follows:

$$f=\begin{cases} f_l=16/\mathrm{Re} & \mathrm{Re}<2100 \\ \left[f_l\times(4000-\mathrm{Re})+f_t\times(\mathrm{Re}-2100)\right]/1900 & 2100\leqslant\mathrm{Re}\leqslant4000 \\ f_t=0.079\times\mathrm{Re}^{-0.25} & \mathrm{Re}>4000 \end{cases} \tag{14}$$

In the calculation of the Reynolds number, the viscosity of the working fluid is determined as:

$$\bar{\mu}=x\mu_v+(1-x)\mu_l \tag{15}$$

The calculation method of the pressure drop in the vapor grooves is the same as that in the vapor line. However, because the mass flowrate of the working fluid increases linearly from zero to the maximum value in the vapor grooves, the vapor groove is evenly divided into several segments, and the pressure drop in the vapor grooves is the sum of the pressure drop in each segments:

$$\Delta P_{vg}=\sum_i \Delta P_{vg,i} \tag{16}$$

For a given heat load, the gravitational pressure difference between the liquid line and vapor line, and the pressure drop in each component of the LHP are strong functions of the liquid mass flowrate at the inlet of the vapor line, which is initially unknown. It is therefore impossible to directly calculate the steady-state operating temperature, whose value should be obtained together with liquid mass flowrate at the inlet of the vapor line simultaneously, as shown in the flowchart, Fig. 3 , including

1) Calculating the heat transfer and pressure drop in each component of the LHP, which is the same as our previous mathematical model [20]..

2) Specifying an initial liquid mass flowrate at the inlet of the vapor line as zero, which is obviously smaller than the actual value.

3) Increasing the liquid mass flowrate at the inlet of the vapor line gradually and calculating the temperature distribution along the loop. The total pressure drop along the loop will be just balanced by the gravitational pressure difference between the liquid line and vapor line. Under this condition, the steady-state operating temperature and liquid mass flowrate at the inlet of the vapor line can be obtained simultaneously.

2.4 Capillarity-gravity co-driven mode

When the heat load applied to the evaporator is larger than the transition heat load, LHP operates in the capillarity-gravity co-driven mode. Under this driving mode, the working fluid in the vapor line is pure vapor, and the capillary forces and gravitational pressure head generated in the liquid line are both driving sources for the circulation of the working fluid along the loop, so the pressure balance equation can be expressed as:

$$\int_{ll} \rho_l \, g \, dH + \Delta P_{cap} = \Delta P_{vg} + \Delta P_{vl} + \Delta P_c + \Delta P_{ll} + \Delta P_{wi} \qquad (17)$$

Under such a mode, the working fluid distribution along the loop is generally the same as the LHP operating with no positive elevation. The calculation of heat transfer and pressure drop in each component, as well as the model solution flowchart, were detailed in our previous mathematical model [20], which is not repeated here.

3. EXPERIMENTAL VALIDATION

3.1 Experimental setup

The experimental system was made of stainless steel except that the wick was made of sintered nickel powder, and Table 1 presents the basic parameters of the components where OD and ID represent the outer and inner diameters respectively. No secondary wick was employed in the ground tests, and the LHP had a bayonet extending to the middle point of the evaporator core. Ammonia was selected as the working fluid due to its excellent thermophysical properties in the temperature range of 0-60 ^{o}C.

Fig.4 shows the experimental setup. In the experiments, heat load applied to the evaporator was provided by a thin-film electric heater with the electric resistance of 20 Ω, attached directly to the evaporator casing symmetrically. The heat load can be adjusted from 0W to 300W by altering the output voltage of the DC power. The condenser line

was mounted on an aluminum cold plate with imbedded coolant channels. Ethanol was used as the coolant for the condenser and circulated by a pump through a refrigerator. The heat sink temperature was maintained at constant values. The entire loop was thermally insulated with a layer of sponge to reduce the parasitic heat load from the ambient.

The data acquisition system was composed of a data logger linked to a PC and the IMPview software was used to display and store the experimental data. Copper/constantan (Type T) thermocouples (TCs) were used to monitor the temperature profile along the loop, and the TC locations are shown in Fig.4. The vapor line was divided into five equal segments by six TCs attached on it; and the condenser line was divided into four equal segments by three TCs attached on it. One additional TC was used to measure the ambient temperature (not shown in Fig. 4).

3.2 Experimental validation and discussions

The comparison of the modeling results with the experimental data is shown in Fig.5 where the operating conditions were maintained as follows: the ambient temperature was 22±1.0℃, the heat sink temperature was -20 ±1.0℃, the compensation chamber was vertically above the evaporator, and the condenser was placed 1.0m higher than the evaporator, i.e. the positive elevation was 1.0m.

As shown in Fig.5, the modeling results of the temperature distribution along the loop are in good agreement with the experimental data both in the gravity driven mode (Q_{ap}=20W) and the capillarity-gravity co-driven mode (Q_{ap}=200W), which confirms the validity of the mathematical model established here. When the LHP was operating in the gravity driven mode, because the working fluid in the vapor line is in the two-phase state, the heat transfer between the working fluid and the ambient is in the form of latent heat, and the working fluid keeps at the saturation temperature when it flows along the vapor line despite experiencing the ambient heating effect, which is verified by

both the modeling and experimental results. However, when the LHP was operating in the capillarity- gravity co-driven mode, because the working fluid in the vapor line is pure vapor, the heat transfer between the working fluid and the ambient is in the form of sensible heat, and the working fluid temperature rises continuously when it flows along the vapor line due to the ambient heating effect, as shown in both the modeling and experimental results.

In Fig.5, there exists certain difference for the temperature at the outlet of the vapor line (TC7) between the modeling results and experimental data that the experimental data are obviously lower than the modeling results especially for the capillary forces and gravity co-driven mode (Qap=200W), because of the heat sink cooling effect through axial heat conduction of the wall, which is not considered in the mathematical model.

4. MODELING RESULTS AND ANALYSIS

4.1 Variation of transition heat load

When LHP is operating under the gravity-assisted attitude, its steady-state operating temperature is strongly dependent on the driving mode, i.e. the gravity driven mode or the capillary forces and gravity co-driven mode, which can be judged by the comparison between the heat load applied to the evaporator and the transition heat load. The transition heat load is influenced by a variety of factors including the operating conditions, the LHP structure parameters as well as the charged working fluid, where the positive elevation and heat sink temperature are two main factors, and Fig.6 shows the positive elevation dependency of the transition heat load at different heat sink temperatures. The operating conditions and structure parameters of the LHP are all the same as those in section 3 except the positive elevation and the heat sink temperature.

As shown in Fig.6, for a fixed heat sink temperature and other operating conditions unchanged, the higher the positive elevation, the larger the transition heat load. That is because the gravitational pressure head generated in the

liquid line increases almost linearly with the positive elevation, and increased mass flowrate is needed to cause sufficient frictional pressure drop to balance the gravitational pressure head, as shown in equation (1). As the transition heat load is nearly proportional to the mass flowrate, and it will increase accordingly. At the same time, the transition heat load first increases almost linearly with the positive elevation, and when it reaches a certain value (about 40W in this study), it begins to increase smoothly. That can be explained as follows: first, the pressure drop in the vapor line and the condenser occupies the major part of the total pressure drop, as shown in Fig.7; second, when the transition heat load is small, the mass flowrate along the loop is very small accordingly, and the flow regime in the vapor line and the condenser is laminar flow that the frictional pressure drop is proportional to the mass flowrate, however, when the transition heat load is comparatively large, the mass flowrate along the loop increases accordingly, and the flow regime in the vapor line and the condenser becomes turbulent flow that the frictional pressure drop is almost proportional to the square of the mass flowrate.

When the transition heat load is small, the effect of heat sink temperature on the transition heat load is not obviously, and the transition heat load curves at different heat sink temperatures almost overlaps. However, when the transition heat load is comparatively large, a higher heat sink temperature results in larger transition heat load. That is because for a comparatively large transition heat load, the LHP will generally operate in the constant conductance mode, a higher heat sink temperature leads to an increased operating temperature. For ammonia, the density of the saturated vapor increases notably with its saturation temperature, and more mass flowrate will be needed to generate sufficient frictional pressure drop to balance the gravitational pressure head generated in the liquid line. Although the evaporative latent heat of ammonia decreases with its saturation temperature, the increase of the mass flowrate is dominant, and the transitional heat load increases accordingly.

4.2 Variation of mass flowrate

When the LHP is operating under horizontal or adverse elevation attitudes, the mass flowrate in the system is nearly proportional to the heat load applied to the evaporator considering the small heat leak from the evaporator to the CC, the heat load for heating the fluid flowing through the wick and the variation of the evaporative latent heat of working fluid with the operating temperature, as shown by equation (7). However, when the LHP is operating under the gravity-assisted attitude, the situation becomes much different.

Fig.8 shows the variation of the mass flowrate with the heat load applied to the evaporator at the inlet of the vapor line when the LHP is operating under the gravity-assisted attitude. The operating conditions and structure parameters of the LHP are all the same as those in section 3.2. As shown in Fig.8, when the LHP is operating under the gravity-assisted attitude, the vapor mass flowrate at the inlet of the vapor line is nearly proportional to the heat load applied to the evaporator both in the gravity driven mode and the capillary forces and gravity co-driven mode. While the liquid mass flowrate at the inlet of the vapor line decreases sharply with the heat load applied to the evaporator in the gravity driven mode, and it reduces to zero at the transition heat load. In the capillary forces and gravity co-driven mode, the liquid mass flowrate at the inlet of the vapor line always keeps at zero. As a result, in the gravity driven mode, the total mass flowrate in the system first decreases with the heat load applied to the evaporator until it reaches the lowest value, then it begins to increase gradually. While in the capillary forces and gravity co-driven mode, the total mass flowrate in the system increases almost linearly with the heat load applied to the evaporator.

When the LHP is operating in the gravity driven mode, the total mass flowrate is obviously larger than that under the horizontal or adverse elevation attitudes due to the additional liquid mass flow in the vapor line, and the cooling of the return liquid to the CC is enhanced considerably as expressed by equation (18):

$$Q_{sub} = \dot{m} C_{pl} (T_{cc} - T_{cc,in}) \quad (18)$$

As shown in equation (18), in the gravity driven mode, first, the total mass flowrate increases obviously; second, the increased mass flowrate in the liquid line could inhibit the temperature rise due to ambient heating effect when the working fluid flows along the liquid line and reduce the working fluid temperature at the inlet of the CC. Both the reasons above contribute to enhanced cooling of the return liquid to the CC. Meanwhile, because the pressure of the working fluid in the CC is almost the same as that in the evaporator, the saturation temperature difference between the evaporator and the CC becomes rather small as well as the radial heat leak from the evaporator to the CC. Both enhanced cooling and reduced heat leak to the CC will result in a much lower steady-state operating temperature. Experimental results confirm the analysis above. As shown in Fig. 9, when the LHP is operating in the gravity driven mode, the steady-state operating temperature is obviously lower than that under the horizontal or adverse elevation attitudes. Whereas when the LHP is operating in the capillary forces and gravity co-driven mode, the steady-state operating temperature is slightly lower than that under the horizontal or adverse elevation attitudes.

4.3 Steady-state operating temperature at different positive elevations

Fig. 10 shows the heat load dependency of the steady-state operating temperature of the LHP at different positive elevations. The ambient temperature is 22℃, and the heat sink temperature is -18℃. The structure parameters of the LHP are all the same as those in section 3.

As shown in Fig.10, when the LHP is operating under the gravity-assisted attitude, the steady-state operating temperature curve is no longer a typical “V” shape, but exhibits unique trend due to the existence of two driving modes. It is easy to find that the higher the positive elevation, the larger the transition heat load, that is quite in agreement with the results in Fig.6. In the gravity driven mode, the steady-state operating temperature first increases

until it reaches a peak value, then it begins to drop gradually. Meanwhile, the positive elevation has great effect on the steady-state operating temperature in the gravity driven mode, i.e. the higher the positive elevation, the lower the steady-state operating temperature; however, the effect of positive elevation on the steady-state operating temperature in the capillary forces and gravity co-driven mode becomes not salient, and the operating temperature curves at different positive elevations almost overlap. The reason is closely associated with the variation of the total mass flowrate in the system as detailed in section 4.2.

4.4 Thermal conductance at different positive elevations

Fig. 11 shows the heat load dependency of the thermal conductance of the LHP at different positive elevations where the thermal conductance is calculated as:

$$G = Q_{ap} / (T_e - T_s) \tag{19}$$

The operating conditions and structure parameters of the LHP are all the same as those in section 4.3.

As shown in Fig.11, when the LHP is operating under the gravity-assisted attitude, there exist two zones: the variable conductance zone where the thermal conductance keeps varying and the constant conductance zone where the thermal conductance changes within a rather narrow range, and this is a typical character of LHPs. However, in the gravity driven mode, the thermal conductance curve exhibits unique trend. When the positive elevation is relatively large, there exists a peak value on the thermal conductance curve, which is quite different from the situation under the horizontal or adverse elevation attitudes. It is easy to find that the positive elevation has great effect on the thermal conductance in the gravity driven mode, i.e. the higher the positive elevation, the larger the thermal conductance; however, the effect of positive elevation on the thermal conductance in the capillary forces and gravity co-driven mode becomes not salient, and the thermal conductance curves at different positive elevations almost

overlap. The results are in agreement with those in section 4.3.

5. CONCLUSIONS

A steady-state mathematical model of a LHP in gravity-assisted operation has been established based on two driving modes: gravity driven mode and capillary forces and gravity co-driven mode. The modeling results show good agreement with the experimental data. Theoretical investigation on the operating principle and characteristics of the LHP under gravity-assisted attitude has been conducted extensively, and the conclusions below have been reached:

- With a fixed positive elevation and other operating conditions unchanged, there exists a transition heat load. When the heat load applied to the evaporator is smaller than the transition heat load, LHP operates in the gravity-driven mode that gravity is the only driving source for the circulation of the working fluid along the loop; otherwise, LHP operates in the capillary forces and gravity co-driven mode that capillary forces and gravity are both driving sources for the circulation of the working fluid along the loop.
- With other operating conditions unchanged, the transition heat load first increases almost linearly with the positive elevation; when it reaches a certain value, it begins to increase slowly.
- When LHP is operating in the gravity driven mode, the working fluid in the vapor line is in the two-phase state due to the existence of additional liquid mass flow, and the total mass flowrate in the loop first decreases quickly to the lowest value, then it begins to increase gradually with the heat load applied to the evaporator, which exhibits unique variation trend and is much different from the situation under horizontal or adverse elevation attitudes.
- When LHP is operating in the gravity driven mode, the operating temperature is obviously lower than that under horizontal or adverse elevation attitudes due to reduced heat leak from the evaporator to the compensation

chamber and enhanced cooling of the return liquid to the compensation chamber; Whereas when LHP is operating in the capillary forces and gravity co-driven mode, the operating temperature is approximate to that under horizontal or adverse elevation attitudes.

- The positive elevation has great effect on the steady-state operating temperature and thermal conductance of the LHP in the gravity driven mode: the higher the positive elevation, the lower the operating temperature, and the larger the thermal conductance; however, in the capillary forces and gravity co-driven mode, the effect of positive elevation can be generally ignored.

ACKNOWLEDGEMENT

This work was supported by Beijing Natural Science Foundation (No. 3144031) and the National Natural Science Foundation of China (No. 51306009). Meanwhile, the authors would like to express our appreciation for the financial support from the EU Marie Curie Actions-International Incoming Fellowships (FP7-PEOPLE-2013-IIF-626576).

REFERENCES

[1] Y.F. Maydanik, Loop heat pipes, Applied Thermal Engineering 25 (2005) 635-657

[2] J. Ku, Operating Characteristics of Loop Heat Pipes, SAE paper, No. 1999-01-2007,1999

[3] G.H. Wang, D. Mishkinis, D. Nikanpour, Capillary heat loop technology: space applications and recent Canadian activities. Applied Thermal Engineering 28 (2008) 284-303

[4] Eric W. Grob, Mission performance of the GLAS thermal control system - 7 years in orbit, AIAA Paper, No.2010-6029, 2010

[5] Jose I. Rodriguez, Arthur Na-Nakornpanom, In-flight performance of the test loop heat pipe heat rejection system – seven years in space, AIAA Paper, No. 2012-3500, 2012

[6] L. Bai, G. Lin, H. Zhang, et al. Operating characteristics of a miniature cryogenic loop heat pipe, International Journal of Heat and Mass Transfer 55 (2012) 8093-8099

[7] L. Bai, G. Lin, H. Zhang, et al. Effect of component layout on the operation of a miniature cryogenic loop heat pipe, International Journal of Heat and Mass Transfer 60 (2013) 61-68

[8] J. Xu, X. Ji, W. Yang, et al., Modulated porous wick evaporator for loop heat pipes: Experiment, International Journal of Heat and Mass Transfer 72 (2014) 163-176

[9] J. Li, F. Lin, D. Wang, et al., A loop-heat-pipe heat sink with parallel condensers for high-power integrated LED chips, Applied Thermal Engineering 56 (1-2) (2013) 18-26

[10] Y.F. Maydanik, M.A. Chernysheva, V.G. Pastukhov, Review: Loop heat pipes with flat evaporators, Applied Thermal Engineering 67 (2014) 294-307

[11] A.L. Phillips, K.L. Wert, Loop Heat Pipe Anti Icing System Development Program Summary, SAE Paper, No. 2000-01-2493, 2000

[12] L. Bai, G. Lin, D. Wen, et al. Experimental investigation of startup behaviors of a dual compensation chamber loop heat pipe with insufficient fluid inventory, Applied Thermal Engineering 29 (2009) 1447-1456

[13] G. Lin, N. Li, L. Bai, et al. Experimental investigation of a dual compensation chamber loop heat pipe, International Journal of Heat and Mass Transfer 53(2010) 3231-3240

[14] M. Mitomi, H. Nagano, Long-distance loop heat pipe for effective utilization of energy, International Journal of Heat and Mass Transfer 77 (2014) 777-784

[15] T. Kaya, T.T. Hoang, J. Ku, Mathematical Modeling of Loop Heat Pipes. AIAA paper, No. 99-0477, 1999

[16] T.T. Hoang, T. Kaya, Mathematical Modeling of Loop Heat Pipes with Two-phase Pressure Drop, AIAA paper, No. 99-3448, 1999

[17] M.L. Parker, Modeling of Loop Heat Pipe with Applications to Spacecraft Thermal Control. Pennsylvania: Faculty of Mechanical Engineering and Applied Mechanics, University of Pennsylvania, United States, 2000

[18] P.A. Chuang, J.M. Cimbala, C.T. Conroy, et al. Comparison of experiments and 1-D steady-state model of a loop heat pipe. Proceedings of IMECE, New Orleans, LA USA, 17-22 November, 2002-33542

[19] V.V. Vlassov, R.R. Riehl, Mathematical model of a loop heat pipe with cylindrical evaporator and integrated reservoir, Applied Thermal Engineering 28(2008) 942-954

[20] L. Bai, G. Lin, H. Zhang, et al. Mathematical modeling of steady state operation of a loop heat pipe, Applied Thermal Engineering 29 (2009) 2643-2654

[21] T. Fang, T. Ming, C.P. Tso, et al. Analysis of non-uniform heat loads on evaporators with loop heat pipes, International Journal of Heat and Mass Transfer 75 (2014) 313-326

[22] L. Bai, G. Lin, D. Wen, Modeling and analysis of startup of a loop heat pipe, Applied Thermal Engineering 30(2010) 2778-2787

[23] P.A. Chuang, J.M. Cimbala, J.S. Brenizer, Experimental and analytical study of a loop heat pipe at a positive elevation using neutron radiography, International Journal of Thermal Sciences 77 (2014) 84-95

[24] L. Bai, G. Lin, H. Zhang, Experimental study on steady state operating characteristics of gravity-assisted loop heat pipes, ACTA AERONAUTICA ET ASTRONAUTICA SINICA 29(5) (2008) 1112-1117 (in Chinese)

NOMENCLATURE

A	cross sectional area (m^2)
C_p	specific heat (J/kg K)
f	frictional factor
g	gravitational acceleration (m/s^2)
G	thermal conductance (W/K)
(G/L)	thermal conductance per unit length (W/K m)
h	enthalpy (J/kg)
H	height (m)
L	length (m)
$\dot{m}$	mass flowrate (kg/s)
P	pressure (Pa)
	perimeter (m)
Q	heat load (W)
S	slip ratio
T	temperature (℃)
v	specific volume (m^3/kg)
x	thermodynamic vapor quality

Greek symbols

α	void fraction
λ	latent heat (J/kg)
τ	shear stress (Pa)
ρ	density (kg/m^3)
μ	dynamic viscosity (Pa s)
θ	tilt angle

Subscript

a	ambient or acceleration
ap	applied
c	condenser
cc	compensation chamber
cap	capillary
e	evaporator or evaporation
f	friction
g	gravity
hl	heat leak
hw	heating the fluid in the wick

in	inlet
l	liquid or laminar
ll	liquid line
s	heat sink
sub	subcooling or subcooled
sat	saturation
t	turbulent
v	vapor
vg	vapor groove
vl	vapor line
vl-a	vapor line and the ambient
wi	wick

Table captions

Table1 Basic parameters of the LHP

Figure captions

Table1 Basic parameters of the LHP

Components		Dimensions
OD/ID×Length of Evaporator		Φ18/16×175mm
OD/ID×Length of Condenser		Φ3/2.2×2000mm
Vapor/liquid line length		2800/2500mm
OD/ID of vapor and liquid line		3/2.2mm
Width/height×number of vapor grooves		1.5/1.2mm×20
Volume of CC		20ml
Charge of working fluid		29.9g
Wick	OD/ID×length	16/8×125mm
	Maximum radius	1.0μm
	Porosity	58.7%
	Permeability	$>5\times10^{-14}m^2$

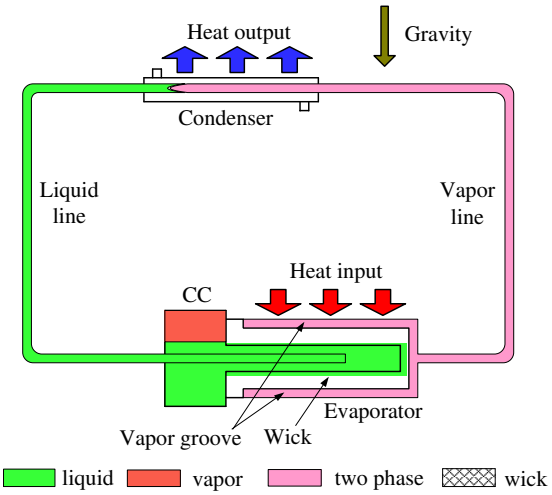

(a) Gravity driven mode

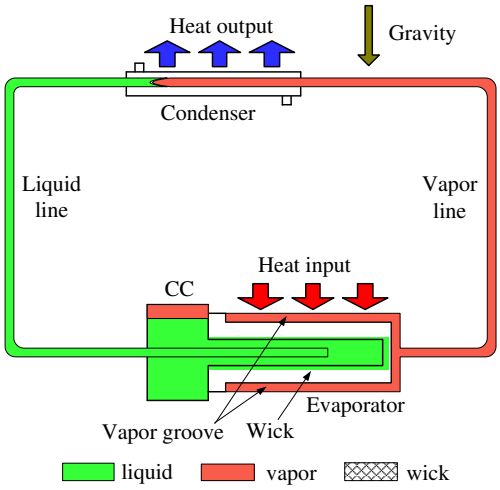

(b) Capillary-gravity co-driven mode

Fig.1 Working fluid distribution inside LHP for different driving modes

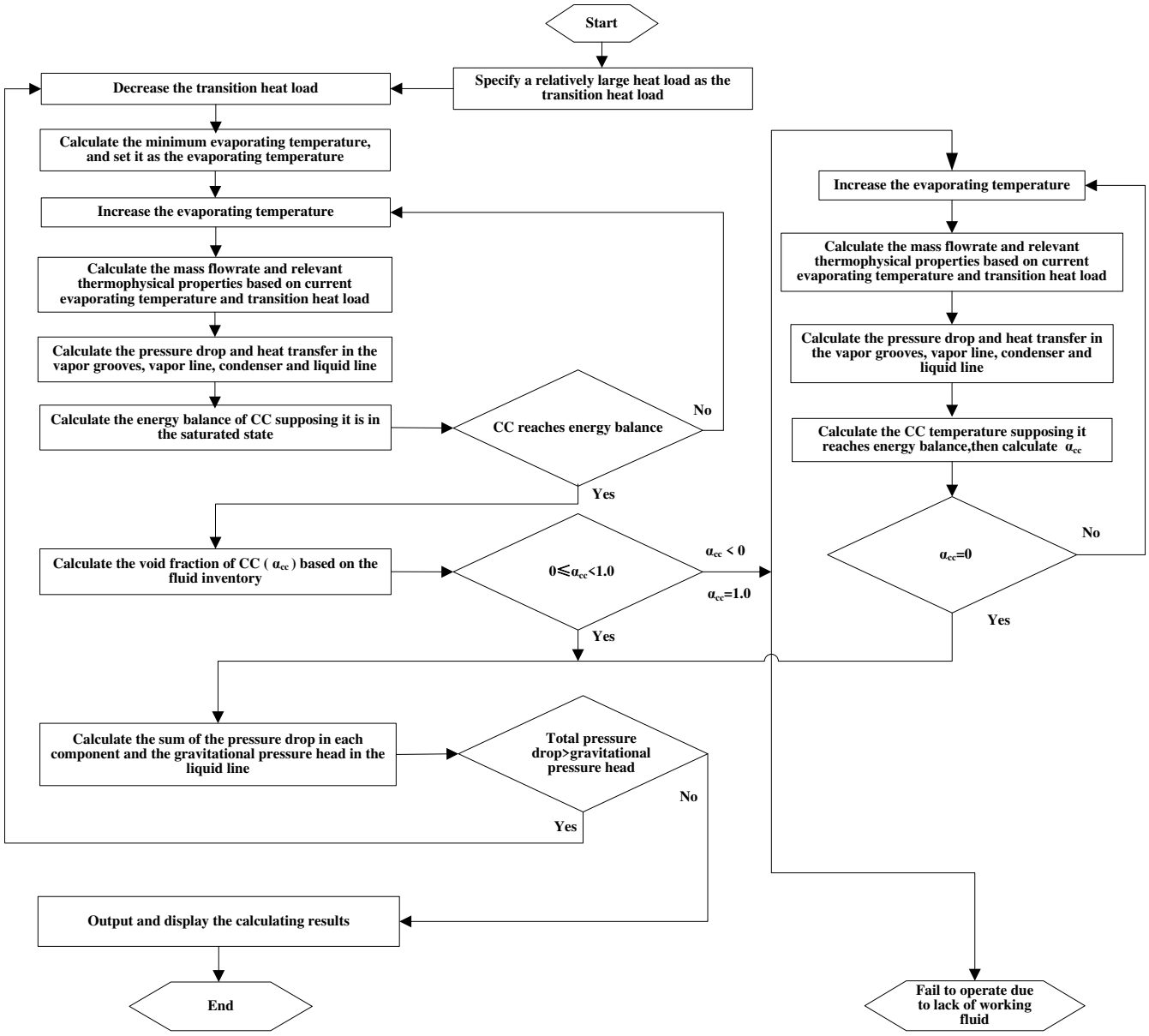

Fig.2 Solution flowchart to determine the transition heat load

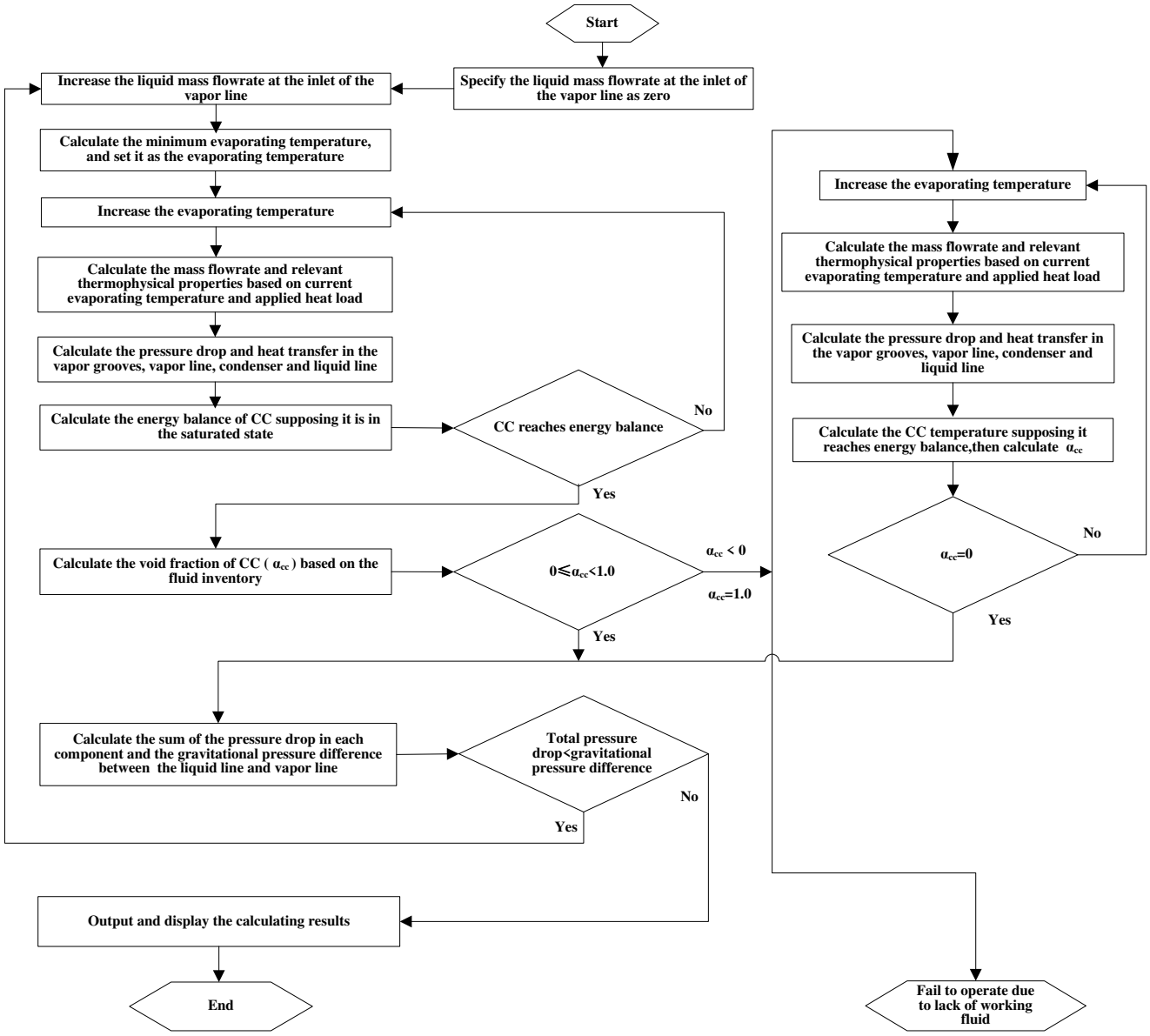

Fig.3 Model solution flowchart for gravity driven mode

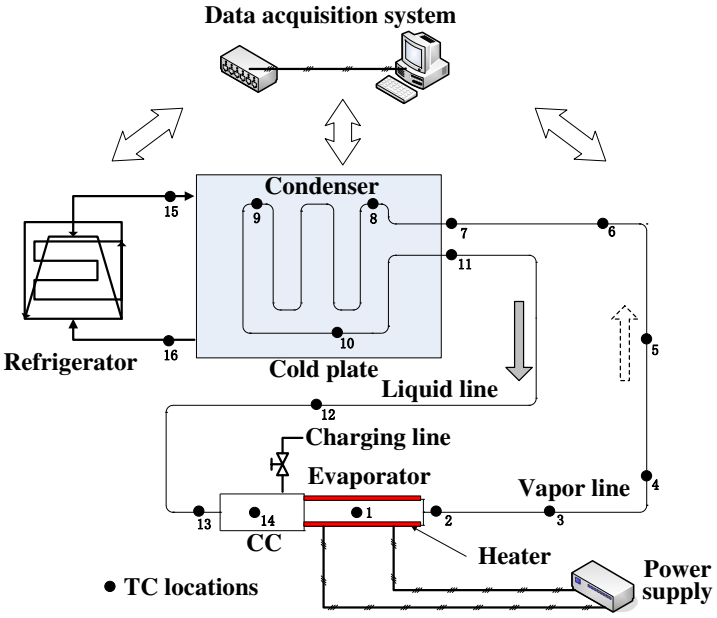

Fig.4 Schematic of the experimental system

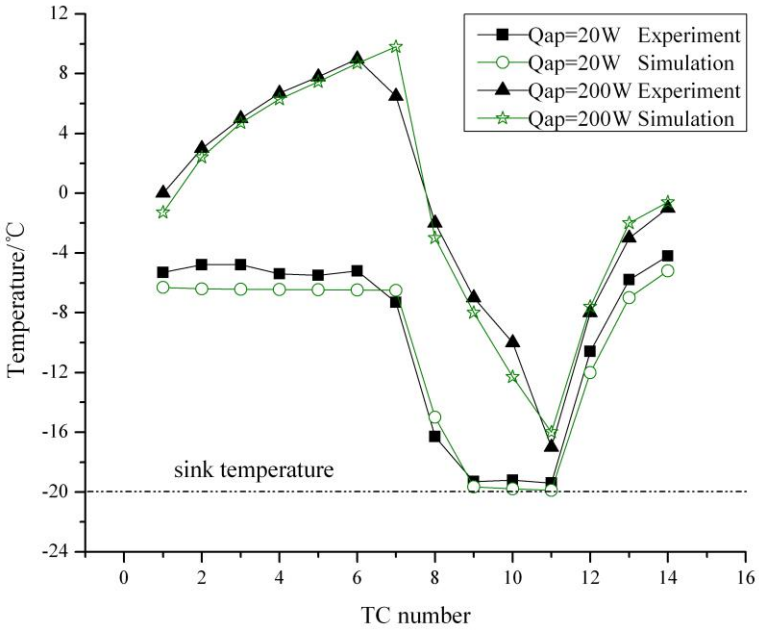

Fig.5 Comparison of the modeling results with experimental data

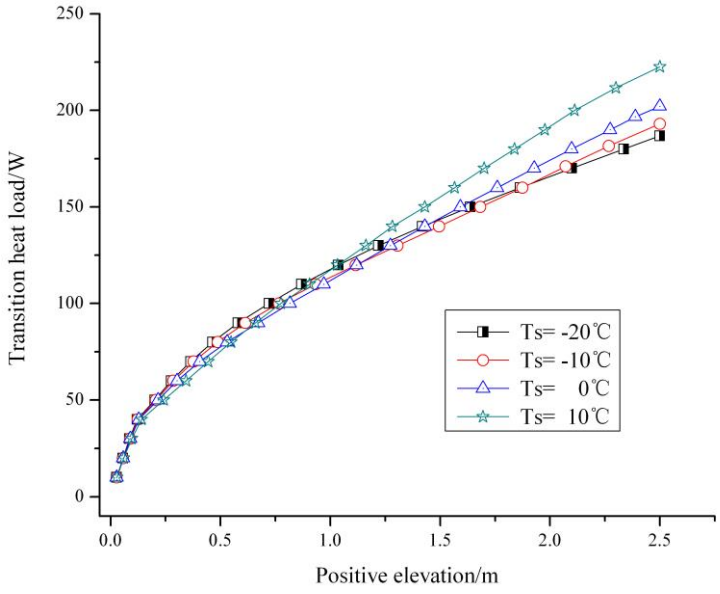

Fig.6 Positive elevation dependency of the transition heat load at different heat sink temperatures

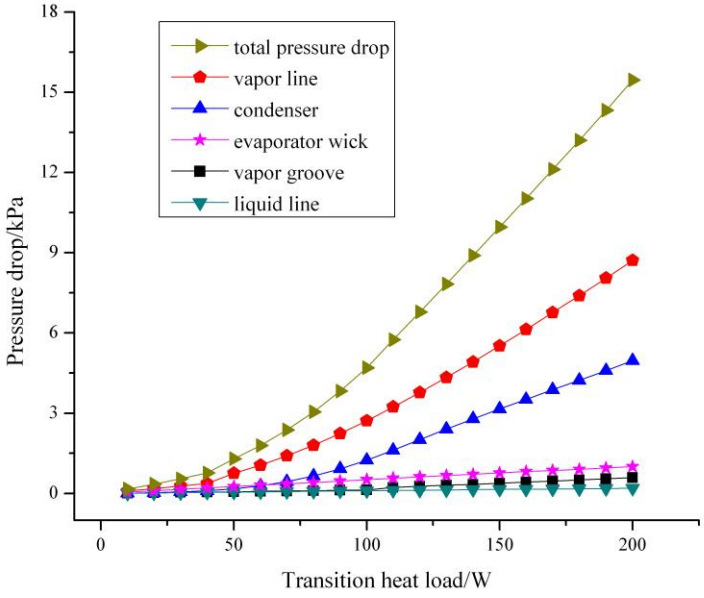

Fig.7 Pressure drop in each component at the transition heat load

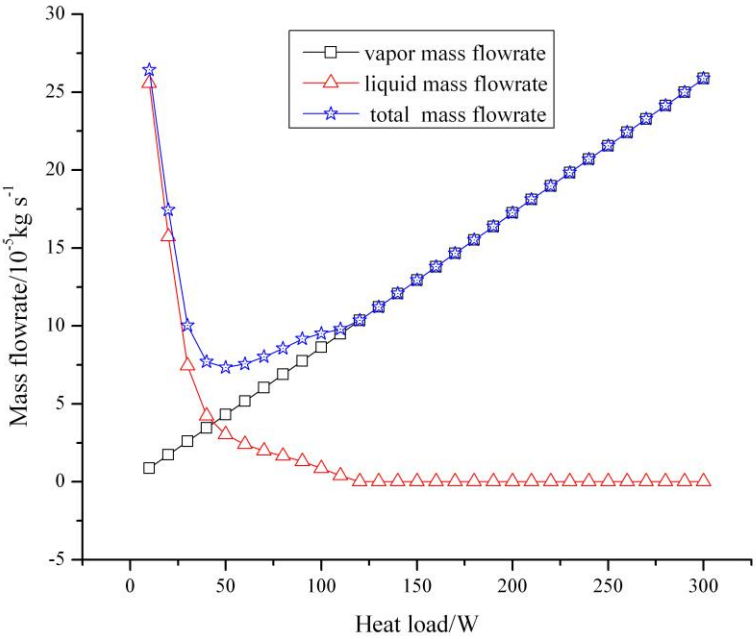

Fig.8 Heat load dependency of the mass flowrate at the inlet of the vapor line

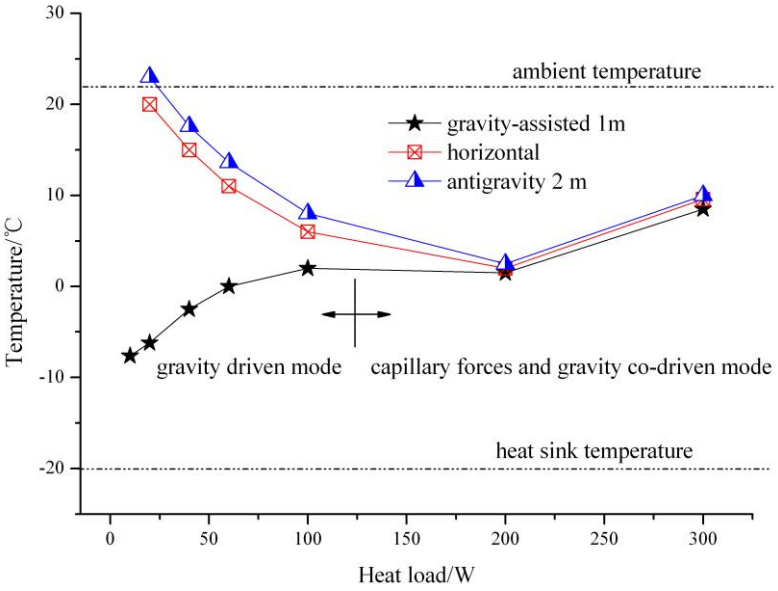

Fig.9 Experimental results of steady-state operating temperature at different attitudes

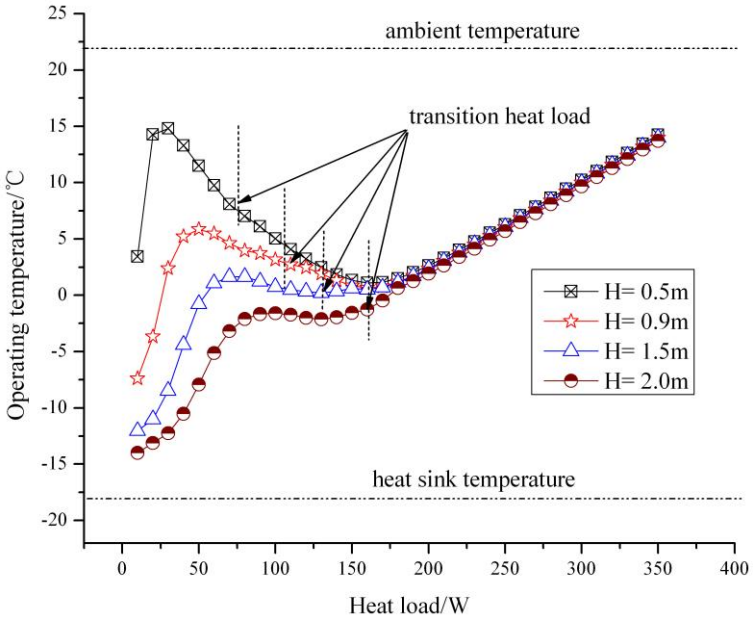

Fig.10 Steady-state operating temperature at different positive elevations

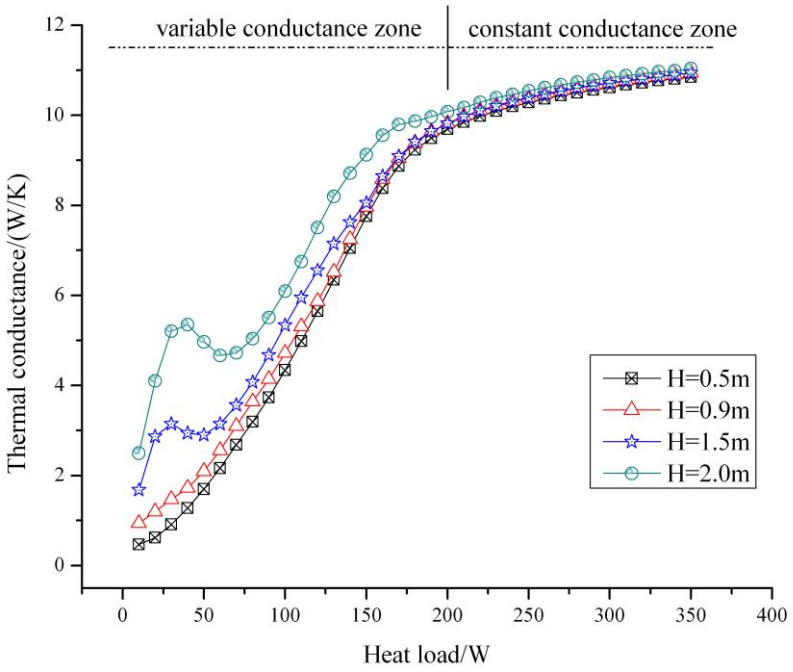

Fig.11 Thermal conductance at different positive elevations